Optical Probing of Spin Polarization of Electrons in Quantum Dot Edge Channels

Shintaro Nomura[1,2,*] and Yoshinobu Aoyagi[2,3]

[1]*CREST, Japan Science and Technology Agency and Institute of Physics, University of Tsukuba Tennodai, Tsukuba, Ibaraki, Japan*
[2]*The Institute of Physical and Chemical Research (RIKEN), Hirosawa, Wako, Saitama, Japan*
[3]*Interdisciplinary Graduate School of Science and Engineering, Tokyo Institute of Technology, Nagatsuda, Midori-ku, Yokohama, Kanagawa, Japan*

(Received 22 March 2004; published 26 August 2004)

We propose an optical method for the investigation of the quantum dot edge channels by utilizing circularly polarized photoluminescence in the integer-quantum-Hall-effect regime. One of the advantages of our method is that the degree of the spin-polarization of the electrons in the inner- and outer-compressible liquids can be probed separately. The observed polarized photoluminescence spectra can be explained by the calculated electron spin-dependent optical transition probabilities based on the local-spin density approximation.

DOI: 10.1103/PhysRevLett.93.096803 PACS numbers: 73.43.–f, 71.15.Mb, 78.55.Cr

It is well known that alternating strips of compressible and incompressible electron liquids are formed at a smooth edge of a 2-dimensional electron system (2DES) [1–5]. The electron density varies gradually from n_s in bulk to 0 at the edge while the potential is constant due to the screening by the electrons, forming the compressible liquid (CL) strip at the edge. The incompressible liquid strips with an even filling factor exist between the CL strips. The properties of these edge channels have been investigated, for example, by transport measurements [6,7], by scanning single-electron transistor microscopy [8,9], and by a photoconductivity measurement [10]. The polarization of the electrons in edge channels has attracted little attention until recently; however, it is now attracting interest in light of the spin control of the electrons. A polarized spin-current was created by locally gating edge channels, which was utilized to polarize nuclear spins [11,12]. When multiple Landau-levels (LLs) are occupied, the polarization of the electrons in the edge channels, however, is not well understood in the existing theories although the polarization is not trivial, especially in the case where the edge state is not defined by a semi-infinite half plane. This is because there exist few experiments that enable a direct probe of the spin-polarization.

A circular polarization-dependent interband spectroscopy is a powerful tool for direct detection of the spin-polarization of electrons in the 2DES. This method has been successfully applied for the investigations of the Skyrmionic excitations at $\nu = 1$ [13–15] as well as the collective excitations of fractional-quantum-Hall (FQH) liquids [16–18]. The relation between the degree of circular polarization of the photoluminescence (PL) and the spin-polarization of the 2DES was parameterized as a function of B/T, where B and T are the external magnetic field and the temperature, respectively [14].

In this Letter, we propose a method to investigate the spin-polarization of the electrons in edge channels in the integer-quantum-Hall (IQH) effect regime. The electron spin-polarization can be directly obtained by the circularly polarized PL spectra. The assignment of the observed peaks in the PL is confirmed by a theoretical calculation based on the local-spin-density approximation (LSDA) [5,19], modeling the edge channels at the filling factor $\nu \approx 3$. Our problem is restricted to the weak magnetic field regime where more than two LLs are occupied. In this regime, we assume that the electron-electron interaction is relatively weak and the LSDA gives a good approximation. Strongly correlated electronic states in quantum dots (QDs) in the regime where the electrons occupy only the single-particle states of the lowest LL were studied using a harmonic oscillator model [20]. We realistically model the electron states and especially the position dependence of the acceptor level for comparison with the PL spectrum of the field-effect lateral QD structure by discritizing the system in 3-dimensional (3D) mesh [19].

The sample used in the present study is based on a molecular-beam epitaxy grown GaAs-$Al_{1-x}Ga_xAs$ ($x \approx 0.3$) single-heterojunction structure. The GaAs capping layer is 7.5 nm thick. The doped and the undoped $Al_{1-x}Ga_xAs$ layer are 30 and 40 nm thick, respectively. The concentration of the donors of the $Al_{1-x}Ga_xAs$ layers is $1 - 2 \times 10^{18}$ cm^{-3}. A Be-δ-doped layer is located 25 nm away from the heterointerface with a nominal doping density of 2×10^{10} cm^{-2}. The 2-dimensional (2D) electron density (n_s) without modulation by the external bias voltage under illumination was estimated to be 3.6×10^{11} cm^{-2} at 1.8 K from an optical Shubnikov-de Haas measurement. A semitransparent Ti/Au Schottky gate structure was fabricated on the surface with square mesh of a period (L_0) of 400 nm and a width of 25 nm by the electron beam lithography [19,21]. A bias voltage (V_B) was applied between the surface mesh gate structure and an Ohmic back-contact on a n-type GaAs substrate. The PL measurements were performed by exciting the sample at 800 nm with a continuous wave Ti:Sapphire laser at the incident power density of

10 mW/cm^2 at 1.8 K. The PL from the sample was dispersed through a 75 cm monochromator and detected by a liquid nitrogen cooled charge-coupled-device detector.

In 2DES at $\nu \approx 3$, three peaks are observed in the PL spectrum due to the principal quantum number $N = 0$ Landau-level (LL0), $N = 1$ Landau-level (LL1), and a shake-up process (SU0), as shown in Fig. 1(a) at 5 T at $V_B = 0$ V. The degree of circular polarization as defined by $P = (I_{\sigma^-} - I_{\sigma^+})/(I_{\sigma^-} + I_{\sigma^+})$, where I_{σ^-} (I_{σ^+}) is the PL intensity of σ^- (σ^+) polarization, is small ($P_0 = 0.60$) for LL0 and large ($P_1 = 0.78$) for LL1 as shown in Fig. 1(b). At $\nu = 3$, the electrons in the fully occupied LL0 are spin unpolarized whereas a fully spin polarized state is realized in the half-filled LL1. The observed P in PL depends on both the electron spins and the population of Zeeman sublevels of the holes. The latter contribution depends on B/T and can be independently determined [14]. Thus, the electron spin-polarization (η) can be estimated from the observed P by using P_0 and P_1 as given by $\eta = (P - P_0)/(P_1 - P_0)$. The estimated η is also depicted in Fig. 1(c). The P of SU0 at $V_B = 0$ V is larger than P of LL0. This result is in agreement with the theory that the SU0 is due to resonant many-body interaction associated with the inter-Landau-level Auger process [22]. By applying a negative bias voltage V_B, with increase in the strength of the confinement potential for electrons, the PL intensity of the LL1 peak is weakened because the number of the electrons in the LL1 decreases. At $V_B = -1.3$ V, the PL from LL1 is identified as a shoulder.

A remarkable feature observed in Fig. 1(a) is that LL0 splits at below $V_B = -0.5 - -0.6$ V. The splitting energy depends on the energy difference of the electrostatic

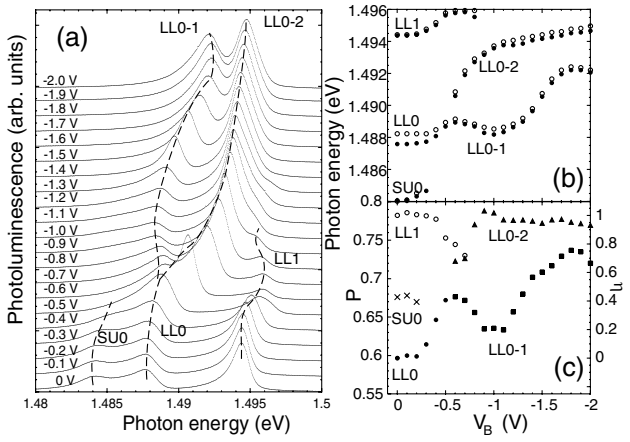

FIG. 1. (a) PL spectra at the bulk filling factor $\nu = 3$ (5 T) between $V_B = 0$ and -2.0 V for σ^- polarization. Zero points of the y axis are shifted for clarity. Dashed curves are a guide for eyes. (b) Optical transition energy of the peaks in PL for σ^- (solid circles) and σ^+ (open circles) polarization. (c) Bias voltage dependence of degree of polarization P of the peaks in PL for LL0 (solid circles), LL1 (open circles), SU0 (crosses), LL0-1 (solid squares) and LL0-2 (solid triangles). The estimated spin-polarization η is also shown.

potential below the surface mesh gate and at the center of a QD. The splitting energy increases from $V_B = -0.6$ to -1.1 V as shown in Fig. 1(b), reflecting the increase of the electrostatic confinement potential. The lower (LL0-1) and the higher (LL0-2) peaks are the emission from the electrons in the inner- and outer-CL regions, respectively, according to a LSDA calculation as described in the following. Further evidence for this assignment is given by the higher polarization P of LL0-2 than that of LL0-1 in Fig. 1(c). P of LL0-2, the outer-CL strip, increases with decrease in V_B between -0.6 and -1.0 V, and at -1.0 V the electrons in LL0-2 are highly polarized. On the contrary, P of LL0-1, the inner-CL region, stays in the range 0.67 and 0.63 between $V_B = -0.6$ and -1.0 V.

The above picture of the separately observed spin polarizations of the inner and outer-CL regions is verified by a calculation based on the LSDA formalism. The density-functional theory has been widely applied to calculate the electronic states of QDs in magnetic field, especially for QDs with electron number $N \approx 30 - 100$, since it is empirically known to give good approximations [4,5,19,23–25]. Here, a 3D mesh of $80 \times 80 \times 8$ and $80 \times 80 \times 30$ per unit cell is used for the calculation of the wave function and the potential, respectively. The magnetic field perpendicular to the heterointerface is taken into account by the gauge-invariant discretization method [26] with the symmetric gauge. A periodic boundary condition is applied laterally. The Hamiltonian is required to be a periodic function of L_0. Thus, only discrete values are allowed for the external magnetic field in our method since a phase factor $\exp[iaL_0/(2l_B^2)]$ is imposed on the Hamiltonian by the gauge-invariant discretization method in the symmetric gauge upon linear transformation of $x \rightarrow x + L_0$ where a and l_B are the period of the mesh for discretization and the magnetic length. The quasi-Fermi energy (E_F) is assumed to be equal to the Fermi energy in the n-type GaAs substrate, which is assumed to be pinned 0.96 eV below the conduction band edge of GaAs at the surface [27]. The bias voltage (V_g) is applied between the quasi-Fermi energy and the surface gate structure. The donor concentration is taken to be 1.63×10^{18} cm^{-3} , which is determined such that the calculation reproduces the filling factor $\nu = 3$ at $V_g = 0$ V and at $B = 4.14$ T , where the imposed phase factor satisfies the required periodicity. Other parameters used in the calculations are the electron effective mass $m_e = 0.0665$, the gyromagnetic factor $g = -0.44$, and the dielectric constant $\epsilon = 12.53$. The residue of the potential is converged to an accuracy of less than 10^{-5} eV. Details of the calculation are described elsewhere [19].

An intuitive picture of the IQH edge state is given by plotting the single-particle energies as a function of the square of the average electron position from the center of a QD ($\mathbf{r}_c$) as defined by $\langle \rho_i^2 \rangle = \int |\mathbf{r} - \mathbf{r}_c|^2 \phi_i^*(\mathbf{r}) \phi_i(\mathbf{r}) d^3\mathbf{r}$, where i is the index of the electron state, as shown in Fig. 2(a). ρ_i^2 is related to the azimuthal rotational quan-

tum number M by $\rho_i^2 = 2l_B^2(M + 1/2)$ in the case of 2DES. The CL region is identified in Fig. 2(a) for $V_g = -0.6$ V in the region $\langle\rho_i^2\rangle < 90l_B^2$, where the electric field is screened. The region $90l_B^2 < \langle\rho_i^2\rangle < 210l_B^2$ is an incompressible liquid strip, and the outer-CL strip is seen at the edge in the region $\langle\rho_i^2\rangle > 210l_B^2$. This ordering of the strips corresponds to the "C state" as denoted by Chklovskii *et al.* [1]. The kink observed at $\langle\rho_i^2\rangle = 251l_B^2$ is due to the size of the unit cell of 400 nm × 400 nm assumed in the calculation. Figure 2(b) shows the electron density distribution and the single-particle potential for up- and down-spin electrons on the plane of maximum electron density. The position of the edge is compared with the edge shown intuitively in Fig. 2(a).

As can be seen from Fig. 2(a), the single-particle energies of LL1 and LL0 outer-CL strip are nearly degenerate. However, they form separate peaks in the interband optical transition spectra where both the electron and hole energies are relevant, unlike the density of states shown in Fig. 2(a). The effective hole potential is a reversal of the effective electron potential excluding the exchange term as defined by $E_{\rm eff}^{(h)}(\mathbf{r}) = -[V_c(\mathbf{r}) + V_H(\mathbf{r})]$, where V_c and V_H are the electrostatic confinement potential and the Hartree term, respectively. Our calculation shows that the effective hole potential is higher at the center of a QD than the edge, which enables separate observation of the interband transition from LL1 and the LL0 outer-CL strip.

The optical transition probability is proportional to [19]

$$J_\sigma(E) = \sum_j \sum_{\mathbf{r}'} \int d^3\mathbf{r}\rho_{j,\sigma}^{(e)}(\mathbf{r})\rho^{(\mathrm{h})}(\mathbf{r},\mathbf{r}') \times\delta\left[E_j^\sigma + E_{\rm eff}^{(\mathrm{h})}(\mathbf{r}') + E_{\rm g} - E\right] \quad (1)$$

where $\rho_{j,\sigma}^{(e)}(\mathbf{r}) = f[(E_{\rm F} - E_j^\sigma)/k_{\rm B}T]|\phi_{j,\sigma}(\mathbf{r})|^2$, $\rho^{(h)}(\mathbf{r},\mathbf{r}') = \delta(\mathbf{r}-\mathbf{r}')$, $T = 2$ K, and E, σ, and E_j^σ are the transition energy, the spin index, and the eigenenergy of the j-th electron state with spin σ, respectively. The band gap energy E_g is taken to be 1.494 eV including the acceptor binding energy. The optical dipole matrix element between an electron and a hole is approximated as unity because of the strong localization of the hole at the acceptor site. The summation with respect to $\mathbf{r}'$, where $\mathbf{r}'$ represents the position of the acceptor atom, is performed on the plane at a fixed distance from the heterointerface. This implies that the optically created holes are trapped at the uniformly distributed acceptors at a constant probability independent of the position.

Three peaks appear in the spectrum J_σ due to LL0 inner-CL, LL0 outer-CL strip, and LL1 inner-CL as shown in Figs. 3(a) and 3(b). The optical transition energy between the LL0 electrons in the outer-CL strip and a hole is lower than the transition energy between the LL1 electrons in the inner-CL and a hole. The essential features of the polarization of the peaks observed in PL are reproduced by the calculation.

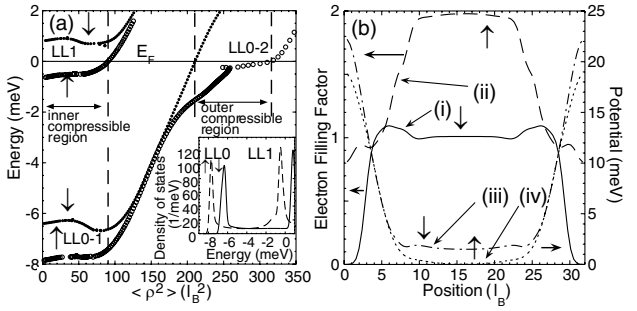

FIG. 2. (a) Single-particle energy plotted against $\langle\rho_i^2\rangle$ at $V_g = -0.6$ V for down- (solid circles) and up- (open circles) spin electrons. (inset) Density of states for down- (solid lines) and up- (dashed lines) spin electrons. (b) Electron density distribution of down-spin electron (i), up-spin electron (ii), and potential of down-spin electron (iii) and up-spin electron (iv) at $V_g = -0.6$ V, along the horizontal direction parallel to the side of the square mesh through the center of the QD. Potential is offset for clarity.

At $V_g = 0$ V, the optical transition probability is proportional to the electron density of states within the single-particle picture since the effective hole potential $E_{\rm eff}^{(h)}(\mathbf{r})$ is constant on the plane of the acceptor cites. At small $|V_g|$, the electrostatic potential gives only small modulation of the single-particle energy and the edge state is not formed.

At V_g just below the threshold voltage for the formation of the edge state, both the up- and down-spin electrons occupy the LL0 outer-CL strip. The polarization of the peak due to the LL0 outer-CL strip is small at $V_g = -0.4$ V. This is observed in PL in Fig. 1 for $V_B = -0.6$ V. With decrease in V_g, the LL0 outer-CL strip for the down-spin electrons is depopulated. The polarization of the peak due to the LL0 outer-CL strip becomes larger at $V_g = -0.5$ V. This is observed in Fig. 1(c) for $V_B = -0.9$ V. Further decrease in V_g results in a decrease in the polarization of the peak due to the LL0 outer-CL strip as shown in Fig. 3(a) for $V_g = -0.6$ and -0.8 V, and disappearance of the well-developed peak due to the LL0 outer-CL strip for both the up- and down-electrons at $V_g \leq -1.0$ V. Corresponding decrease of the polarization is observed in Fig. 1 for $V_B \leq -0.9$ V. The increase of the splitting energy between the inner- and outer-CLs with decrease in V_g between -0.4 V and -0.6 V agrees with the observation in Fig. 1(c) for V_B between -0.6 and -1.0 V.

While our model calculation explains essential features of our experimental observations, there remain small discrepancies. In the PL spectra in Fig. 1, the peak due to LL1 disappears before the peak due to the LL0 outer-CL strip disappears with decrease in V_B. A contradictory dependence on V_g is seen in Fig. 3. The increase of P of LL0-1 in Fig. 1(b) at $V_B \leq -1.2$ V

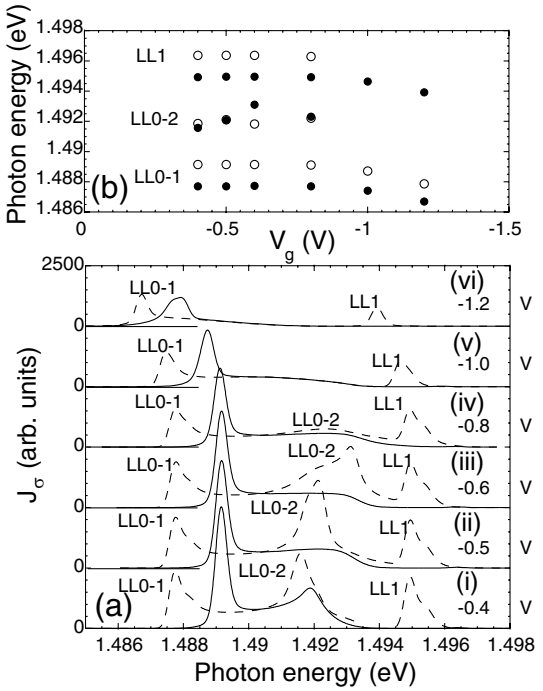

FIG. 3. (a) Calculated optical transition probability J_σ at (i) $V_g = -0.4$, (ii) -0.5, (iii) -0.6, (iv) -0.8, (v) -1.0, and (vi) -1.2 V. Solid and dashed lines depict J_σ for the down and up spins, respectively. (b) V_g dependence of the peak energies in J_σ for up- (solid circles) and down-spin (open circles) electrons, respectively.

contradicts with the calculated results for $V_g \leq -1.0$ V. These discrepancies may be attributed to the following reasons. First, the PL is measured at 5 T, but the calculation is performed at 4.14 T due to the constraint of the phase factor by the boundary condition described before. Since the size of the system is effectively smaller for the calculation than the experiment if the size is measured with l_B, the bias voltage range for the outer-CL strip to be formed is narrower for the calculation. Second, the sublevels of the hole state are not taken into account in the calculation. The observed increase of the circular polarization for large $|V_B|$ may be attributed to the change in the hole sublevels by the electrostatic potential. The third possible reason is deviation of V_B from V_g for large $|V_B|$, although it is often considered to be reasonable that the quasi-Fermi energy of the electrons matches to the Fermi energy of heavily n-doped GaAs substrate at an equilibrium condition. While further development of the technique in the theoretical modeling may be necessary for more quantitative arguments, the bias voltage dependencies of the PL lineshapes and the degrees of circular polarization are remarkably well explained by the calculated spectra, which confirms the feasibility of our proposed method.

In summary, the electron spin-polarization of the CL strips in the IQH-effect regime is separately detected by the circularly polarized PL measurements, and the experimental results are verified by our model calculation based on LSDA. Our proposed method may also be applied to experimental study of the edge channels for the FQH-effect regime. With a combination of the near-field scanning optical microscopy [28], our method is expected to enable us to spatially map the polarization of the electrons in edge channels. Such an experiment is under preparation.

We would like to acknowledge fruitful discussions with G. E. W. Bauer, T. Nakanishi, J. Nitta, T. Saiki, and H. Tamura. Computational support by the Computer Center of RIKEN is gratefully acknowledged. Part of this work was supported by University of Tsukuba Nano-science Special Project.

*Electronic address: snomura@sakura.cc.tsukuba.ac.jp

[1] D. B. Chklovskii, B. I. Shklovskii, and L. I. Glazman, Phys. Rev. B **46**, 4026 (1992).
[2] V. G. Burnett, A. L. Efros, and F. G. Pikus, Phys. Rev. B **48**, 14365 (1993).
[3] L. Brey, J. J. Palacios, and C. Tejedor, Phys. Rev. B **47**, 13884 (1993).
[4] K. Lier and R. R. Gerhardts, Phys. Rev. B **50**, 7757 (1994).
[5] T. H. Stoof and G. E. W. Bauer, Phys. Rev. B **52**, 12143 (1995).
[6] B. W. Alphenaar *et al.*, Phys. Rev. Lett. **64**, 677 (1990).
[7] L. P. Kouwenhoven *et al.*, Phys. Rev. Lett. **64**, 685 (1990).
[8] M. J. Yoo *et al.*, Science **276**, 579 (1997).
[9] A. Yacoby *et al.*, Solid State Commun. **111**, 1 (1999).
[10] R. J. F. van Haren, F. A. P. Blom, and J. H. Wolter, Phys. Rev. Lett. **74**, 1198 (1995).
[11] D. C. Dixon *et al.*, Phys. Rev. B **56**, 4743 (1997).
[12] T. Machida, T. Yamazaki, and S. Komiyama, Appl. Phys. Lett. **80**, 4178 (2003).
[13] E. H. Aifer, B. B. Goldberg, and D. A. Broido, Phys. Rev. Lett. **76**, 680 (1996).
[14] I. V. Kukushkin, K. v. Klitzing, and K. Eberl, Phys. Rev. B **55**, 10607 (1997).
[15] J. L. Osborne *et al.*, Phys. Rev. B **58**, R4227 (1998).
[16] B. B. Goldberg *et al.*, Surf. Sci. **196**, 209 (1988).
[17] I. V. Kukushkin *et al.*, Phys. Rev. Lett. **72**, 736 (1994).
[18] C. Schuller *et al.*, Phys. Rev. Lett. **91**, 116403 (2003).
[19] S. Nomura and Y. Aoyagi, Surf. Sci. **529**, 171 (2003).
[20] P. Hawrylak, A. Wojs, and J. A. Brum, Phys. Rev. B **54**, 11397 (1996).
[21] S. Nomura, T. Nakanishi, and Y. Aoyagi, Phys. Rev. B **63**, 165330 (2001).
[22] P. Hawrylak and M. Potemski, Phys. Rev. B **56**, 12386 (1997).
[23] A. Kumar, S. E. Laux, and F. Stern, Phys. Rev. B **42**, 5166 (1990).
[24] M. Stopa, Phys. Rev. B **54**, 13767 (1996).
[25] K. Hirose, F. Zhou, and N. S. Wingreen, Phys. Rev. B **63**, 075301 (2001).
[26] M. Governale and C. Ungarelli, Phys. Rev. B **58**, 7816 (1998).
[27] A. Kawaharazuka *et al.*, Phys. Rev. B **63**, 245309 (2001).
[28] K. Matsuda *et al.*, Phys. Rev. Lett. **91**, 177401 (2003).